LC mixture with promoted electro-optical properties for LCD applications by using a highly UV-resistant dopant

Shih-Hsien Liu, Po-Jen Yang, and Hong-Cheu Lin*

Department of Materials Science and Engineering, National Chiao Tung University, Hsinchu 300, Taiwan
**linhc@mail.nctu.edu.tw*

Abstract: A highly ultraviolet (UV)-resistant dopant **3HBBTfV** consisting of an α-trifluomethyl vinylbenzene (**TfV**) moiety was synthesized and mixed with a commercial LC host (**A**) to promote its dielectric anisotropy in LC mixture **C** (**A**:**3HBBTfV** = 9:1 w/w). Their electric-optical properties were studied and compared with those of an analogous commercial LC mixture **B** composed of LC mixture **A** (as a commercial host) mixed with the same weight ratio (10% wt.) of a commercial component **3HBEBTf** containing a 3,4,5-trifluorobenzene (**BTf**) moiety. The electro-optical properties of voltage holding ratio (VHR) values and voltage-transmission (*V-T*) curves of LC mixture **C** were sustained after the UV irradiation. These results showed that dopant **3HBBTfV** (acting as an UV stabilizer) demonstrated a higher stability under UV exposure in contrast to commercial component **3HBEBTf**. Therefore, LC mixture **C** (containing UV-resistant dopant **3HBBTfV**) exhibited good UV resistance, high dielectric anisotropy, and excellent electro-optical properties.

OCIS codes: (230.3720) Liquid-crystal devices; (160.3710) Liquid crystals; (120.5050) Phase measurement; (120.6780) Temperature.

References and links

1. Y. H. Jeonga, Y. J. Lima, E. Jeonga, W. G. Jangb, and S. H. Leeb, "Optimal pixel design for low driving, single gamma curve and single cell-gap transflective fringe-field switching liquid crystal display," Liq. Cryst. **35**(2), 187–194 (2011).
2. H. Nam and S. W. Lee, "Low-power liquid crystal display television panel with reduced motion blur," IEEE Trans. Consum. Electron. **56**(2), 307–311 (2010).
3. P. Liu, F. Zafar, and A. Badano, "The effect of ambient illumination on handheld display image quality," J. Digit. Imaging **27**(1), 12–18 (2014).
4. S. Yamada, Y. Hirata, R. Ishii, and T. Ogawa, "Visual evaluation and usefulness of medical high-resolution liquid-crystal displays with use of independent sub-pixel driving technology," Radiological Phys. Technol. **4**(2), 128–133 (2011).
5. S. Y. Lu and L. C. Chien, "Electrically switched color with polymer-stabilized blue-phase liquid crystals," Opt. Lett. **35**(4), 562–564 (2010).
6. M. Schadt and W. Helfrich, "Voltage-dependent optical activity of a twisted nematic liquid crystal," Appl. Phys. Lett. **18**(4), 127–128 (1971).
7. M. Oh-e and K. Kondo, "Electro-optical characteristics and switching behavior of the in-plane switching mode," Appl. Phys. Lett. **67**(26), 3895–3897 (1995).
8. K. Ohmuro, S. Kataoka, T. Sasaki, and Y. Koike, "Development of super-high image quality vertical alignment mode LCD," Dig. Tech. Pap. **28**, 845–848 (1997).
9. I. H. Yu, I. S. Song, J. Y. Lee, and S. H. Lee, "Intensifying the density of a horizontal electric field to improve light efficiency in a fringe-field switching liquid crystal display," J. Phys. D Appl. Phys. **39**(11), 2367–2372 (2006).
10. T. N. Oo, T. Mizunuma, Y. Nagano, H. Ma, Y. Ogawa, Y. Haseba, H. Higuchi, Y. Okumura, and H. Kikuchi, "Effects of monomer/liquid crystal compositions on electro-optical properties of polymer-stabilized blue phase liquid crystal," Opt. Mater. Express **1**(8), 1502–1510 (2011).
11. Y. Chen and S. T. Wu, "Recent advances on polymer-stabilized blue phase liquid crystal materials and devices," J. Appl. Polym. Sci. **131**(13), 40556 (2014).
12. I. H. Chiang, C. J. Long, H. C. Lin, W. T. Chuang, J. J. Lee, and H. C. Lin, "Broad ranges and fast responses of single-component blue-phase liquid crystals containing banana-shaped 1,3,4-oxadiazole cores," ACS Appl. Mater. Interfaces **6**(1), 228–235 (2014).
13. Z. Raszewski, W. Piecek, L. Jaroszewicz, L. Soms, J. Marczak, E. Nowinowski-Kruszelnick, P. Perkowski, J. Kedzierski, E. Miszczyk, M. Olifierczuk, P. Morawiak, and R. Mazur, "Laser damage resistant nematic liquid

#232681 - $15.00 USD Received 16 Jan 2015; revised 26 Feb 2015; accepted 1 Mar 2015; published 12 Mar 2015

crystal cell," J. Appl. Phys. **114**(5), 053104 (2013).
14. Y. J. Park, H. J. Kim, D. S. Park, and I. K. Sung, "Reliability of liquid crystal cell and immiscibility between dual-curable adhesives and liquid crystal," Eur. Polym. J. **46**(7), 1642–1648 (2010).
15. M. Schadt, "Field-effect liquid-crystal displays and liquid-crystal materials: key technologies of the 1990s," Displays **13**(1), 11–34 (1992).
16. M. Mizusaki, Y. Yoshimura, Y. Yamade, and K. Okamoto, "Analysis of ion behavior affecting voltage holding property of liquid crystal displays," Jpn. J. Appl. Phys. **51**(1), 014102 (2012).
17. P. Kumar, S. W. Kang, and S. H. Lee, "Advanced bistable cholesteric light shutter with dual frequency nematic liquid crystal," Opt. Mater. Express **2**(8), 1121–1134 (2012).
18. Y. J. Lim, I. H. Jeong, H. S. Kang, S. Kundu, M. H. Lee, and S. H. Lee, "Reduction of the residual DC in the photoaligned twisted nematic liquid crystal display using polymerized reactive mesogen," Appl. Phys. Express **5**(8), 081701 (2012).
19. L. Lu, A. Bhowmik, and P. Bos, "The effect of dielectric constant on ion adsorption in liquid crystal devices," Liq. Cryst. **40**(1), 7–13 (2013).
20. C. H. Wen, S. Gauza, and S. T. Wu, "Ultraviolet stability of liquid crystals containing cyano and isothiocyanato terminal groups," Liq. Cryst. **3**(11), 1479–1485 (2004).
21. S. Saito and H. Yamamoto, "Transient behavior of field-induced reorientation in variously oriented nematic liquid crystals," Jpn. J. Appl. Phys. **17**(2), 395–406 (1978).
22. K. Tarumi, U. Finkenzeller, and B. Schuler, "Dynamic behaviour of twisted nematic liquid crystals," Jpn. J. Appl. Phys. **31**(1), 2829–2836 (1992).
23. P. Kirsch and M. Bremer, "Nematic liquid crystal for active matrix displays: Molecular design and synthesis," Angew. Chem. Int. Ed. **39**(23), 4216–4235 (2000).
24. D. Pauluth and K. Tarumi, "Advanced liquid crystals for television," J. Mater. Chem. **14**(8), 1219–1227 (2004).
25. M. Bremer, P. Kirsch, M. Klasen-Memmer, and K. Tarumi, "The TV in your pocket: Development of liquid-crystal materials for the new millennium," Angew. Chem. Int. Ed. Engl. **52**(34), 8880–8896 (2013).
26. M. Hird, "Fluorinated liquid crystals-properties and applications," Chem. Soc. Rev. **36**(12), 2070–2095 (2007).
27. I. K. Huh and Y. B. Kim, "New low viscosity liquid crystal compounds containing the 2,3,4-trifluorophenyl moiety for active matrix displays," Liq. Cryst. **29**(10), 1265–1273 (2002).
28. K. Araya, D. A. Dunmur, M. C. Grossel, G. R. Luckhurst, S. E. Marchant-Lane, and A. Sugimura, "Flexible dimers as dopants for liquid crystal display mixtures with faster relaxation times," J. Mater. Chem. **16**(48), 4675–4689 (2006).
29. A. C. Chen, P. C. Huang, S. H. Liu, and K. L. Cheng, "Novel LC materials toward the faster response time and lower driving voltage," In Proceedings of the 14th International Display Workshops *(IDW '07)* **1–3**, 383–386 (2007).
30. Y. Garboyskiy, J. R. Baptist, J. Thomposon, T. Hunter, J. H. Lim, S. G. Min, J. B. Wily, L. M. Malkinski, A. Glushenko, and Z. Celinski, "Increasing the switching speed of liquid crystal devices with magnetic nanorods," Appl. Phys. Lett. **101**(18), 181109 (2012).
31. Y. Kubo, F. Takeshita, T. Matsushita, E. Nakagawa, and T. Kondo, "Liquid crystal composition and liquid crystal display device," European Patent 0, 832, 955 (April 1, 1998).
32. K. Miyazawa, T. Kato, Y. Kubo, and K. Terashima, "Liquid crystal compounds having bis(trifluoromethyl)phenyl rings, liquid crystal compositions and liquid crystal display devices," European Patent 1, 245, 660 (February 23, 2005).
33. S. T. Wu, E. Ramos, and U. Finkenzeller, "Polarized UV spectroscopy of conjugated liquid crystals," J. Appl. Phys. **68**(1), 78–85 (1990).
34. M. Schadt, "Liquid crystal materials and liquid crystal displays," Annu. Rev. Mater. Sci. **27**(1), 305–379 (1997).
35. M. Oh-e, Y. Umeda, M. Ohta, S. Aratani, and K. Kondo, "Unusual voltage-holding ratio characteristics using in-plane switching of nematic liquid crystals," Jpn. J. Appl. Phys. **36**(Part 2, No. 8A), L1025–L1028 (1997).
36. P. T. Lin, S. T. Wu, C.-Y. Chang, and C.-S. Hsu, "UV stability of high birefringence liquid crystals," Mol. Cryst. Liq. Cryst. (Phila. Pa.) **411**(1), 1285–1295 (2004).
37. A. Banerjee and D. E. Falvey, "Direct photolysis of phenacyl protecting groups studied by laser flash photolysis: An excited state hydrogen atom abstraction pathway leads to formation of carboxylic acids and acetophenone," J. Am. Chem. Soc. **120**(12), 2965–2966 (1998).

1. Introduction

Recently, liquid crystal displays (LCDs) are very important and indispensable to modern life owing to their various applications, such as notebooks, monitors, mobile phones, televisions, and portable devices. Due to their small sizes, light weights, portabilities, high image qualities, and low-power consumptions, LCDs have become main trends in all display areas [1–5]. The major ones should be twisted nematic [6], in-plane-switching [7], multi-domain vertical alignment [8], and fringing field switching modes [9]. Currently, nematic liquid crystal (LC) mixtures have been widely utilized in the field of LCDs, and blue phase LCs have potentials to be further explored as new materials for future applications [10–12]. To achieve the reliable request of liquid crystals (LCs) for display applications, the primary concern of stability for LC materials is as important as their

#232681 - $15.00 USD Received 16 Jan 2015; revised 26 Feb 2015; accepted 1 Mar 2015; published 12 Mar 2015

performance. In order to satisfy the requirements of long operational life time and high image quality for the commercial specifications of LCDs, LC materials possessing ultraviolet (UV) resistance also play an important role to reach the long term reliability of the displays [13–15]. In most practical cases, UV irradiation causes gradual degradations of LC molecules. Once LC mixtures are deteriorated by the exposure of UV light, the electro-optical (EO) performance of the LC materials might also be declined. Therefore, the promising LC materials with excellent UV-resistant properties may offer enduring stabilities for display devices. The reliabilities of LCDs can be evaluated by two of the major display performance parameters, including voltage holding ratio (VHR) and residual direct current (RDC) [16–19]. Typically, the durable stabilities of LC mixtures can be estimated by the variations of the VHR and RDC parameters before and after UV treatments [20].

On the other hand, the key requirements of LCDs with high performance must have not only good chemical and thermal stabilities of LC materials, but also involve low viscosities lead to short addressing time and low threshold voltages in displays. Towards fast responsive LCDs, the rotational viscosities of LC materials were known as one of the most important physical properties. For such planar cells, the switching time is proportional to the rotational viscosity coefficient (γ_1) of the LC materials, where a lower rotational viscosity could effectively decrease both rising time (τ_r) and falling time (τ_f), which are given by the following Eqs. (1) and (2) [21–24]:

$$\tau_r = \frac{\gamma_1 d^2}{\pi^2 K_{11}} \left(\frac{|\varepsilon_a|}{\pi^2 K_{11}} V^2 - 1 \right)^{-1} \tag{1}$$

and

$$\tau_f = \frac{\gamma_1 d^2}{\pi^2 K_{11}} \tag{2}$$

where d is the thickness of the LC film, ε_a is the anisotropy of dielectric susceptibility, V is the applied voltage, and K_{11} is the elastic constant of splay. Many previous papers have reported that the molecular structures of LC materials could be adjusted to have low viscosities and high dielectric anisotropies, which were sufficient to be used as the fast responsive LC mixtures [25–30].

A poor UV-resistant performance of a commercial LC mixture **B** consisting of a LC mixture **A** (as a commercial host) mixed with 10% wt. of a commercial component **3HBEBTf** (see Fig. 1) has been reported previously [31,32], which needs to be improved due to the requirement of photo-alignment under UV process. Due to the un-stable ester linkage [23] of the commercial component **3HBEBTf** under UV exposure, LC mixture **A** (removal of component **3HBEBTf**) as a commercial host was used in this study. In addition, the strong absorption bands ca. 254 nm of the two longest conjugated analogous terphenyl compounds in this commercial LC mixture **A** (as a commercial host listed in Table 1) have been reported previously [33], which also un-stabilize LC host **A** under UV exposure. Herein, as demonstrated in Fig. 1 we developed a highly UV-resistant dopant material **3HBBTfV** consisting of an α-trifluomethyl vinylbenzene (**TfV**) moiety to be mixed with the commercial host LC mixture **A** (as a commercial host) to form a LC mixture **C** (**A**:**3HBBTfV** = 9:1 w/w). As illustrated in Fig. 2, the UV resistant dopant **3HBBTfV** was designed and synthesized by a four-step synthesis to produce a phenylcyclohexane derivative containing an α-trifluomethyl vinylbenzene moiety (acting as a molecular dipole moment enhancing component to induce a higher dielectric anisotropy). The mesogenic core (phenylcyclohexane unit) of dopant **3HBBTfV** has a chemical structure similar to those major components in LC host **A**, so it (acting as an UV stabilizer) could be miscible with the LC host at such a high ratio (10% wt.). In contrast to the commercial LC mixture **B** containing 10% wt. of the commercial component **3HBEBTf**, the electro-optical properties of LC mixture **A** (a commercial host) and UV-resistant LC mixture **C** (containing 10% wt. of our newly designed dopant **3HBBTfV**) are compared in this study. LC mixture **C**

#232681 - $15.00 USD Received 16 Jan 2015; revised 26 Feb 2015; accepted 1 Mar 2015; published 12 Mar 2015

containing dopant **3HBBTfV** revealed good UV resistance in voltage holding ratio (VHR) values and voltage-transmission (*V-T*) curves, so its excellent electro-optical properties can improve the performance of the LC mixture in the LCD application.

3HBBTfV **3HBEBTf**

Fig. 1. Structures of the UV-resistant dopant **3HBBTfV** and the commercial compoent **3HBEBTf**.

Table 1. Chemical Structures and Composition of LC Mixture A (Host)

Chemical structure	Weight ratio (wt%)
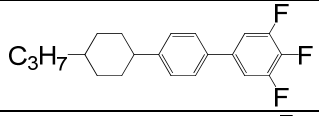	10
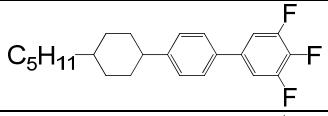	10
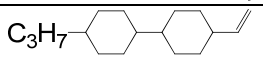	30
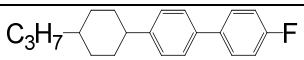	10
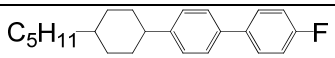	10
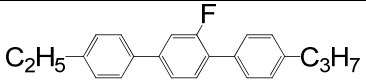	10
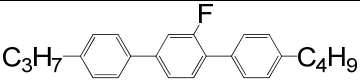	10
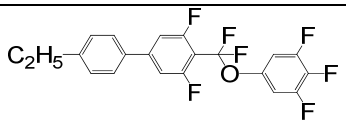	10

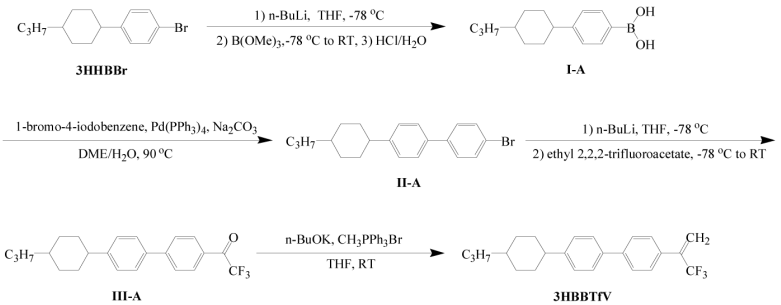

Fig. 2. Synthesis route of dopant **3HBBTfV**

2. Experiments

2.1. Materials

Chemicals and solvents were reagent grades and purchased from Aldrich, Acros, and TCI Co. Tetrahydrofuran (THF) and dichloromethane (DCM) were distilled to keep anhydrous

#232681 - $15.00 USD Received 16 Jan 2015; revised 26 Feb 2015; accepted 1 Mar 2015; published 12 Mar 2015

before use. The other chemicals were used without further purification. Commercial component 3HBEBTf (Tm = 98.0°C) was purchased from Suzhou chemical Co. and as supplied.

2.2. Synthesis

*Synthesis of **I-A***. *n*-BuLi (14.8 mL, 2.5 M in hexane, 35.6 mmol) was added dropwise into a solution of commercially available starting material **3HHBBr** (5.0 g, 17.8 mmol) in anhydrous THF, and the mixture was reacted continuously at −78°C for 1.5 h under nitrogen atmosphere. Then, trimethyl borate (5 mL, 44.5 mmol) was added dropwise to the solution, and the reaction mixture was warmed to room temperature and stirred overnight. The resulting mixture was quenched with 6N HCl and extracted with dichloromethane. The combined organic layers were washed with water and dried over Na_2SO_4 and evaporated. The residual product was purified by flash column chromatography (silica gel, DCM/ethyl acetate = 4:1, v/v) to give **I-A** in a yield of 68% as a white powder. ^{1}H NMR (400 MHz, $CDCl_3$) δ (ppm): 0.92 (m, 3H), 0.96-1.18 (m, 2H), 1.29-1.37 (m, 4H), 1.46-1.56 (m, 3H), 1.89-1.96 (m, 4H), 2.02 (br, 2H), 2.73 (m, 1H), 7.30 (d, *J* = 8.0 Hz, 2H), 7.67 (d, *J* = 8.0 Hz, 2H).

*Synthesis of **II-A***. A solution of **I-A** (3.9 g, 15.8 mmol), 1-bromo-4-iodobenzene (4.07 g, 14.4 mmol), $Pd(PPh_3)_4$ (832 mg, 0.72 mmol), and Na_2CO_3 (12.2 g, 11.5 mmol) in a mixture of 1,2-dimethoxyethane (100 mL) and water (66.7 mL) was stirred at 90°C for 12 h under nitrogen atmosphere. After that, the mixture was cooled to room temperature and extracted with DCM. The combined organic layers were washed with water and dried over Na_2SO_4 and evaporated. The residual product was purified by flash column chromatography (silica gel, hexane/DCM = 5:1, v/v) to give **II-A** in a yield of 59% as a white powder. ^{1}H NMR (400 MHz, $CDCl_3$) δ (ppm): 0.92 (m, 3H), 0.96-1.18 (m, 2H), 1.29-1.37 (m, 4H), 1.38-1.57 (m, 3H), 1.84-1.96 (m, 4H), 2.70 (m, 1H), 7.30 (d, *J* = 8.0 Hz, 4H), 7.53 (d, *J* = 7.4 Hz, 2H), 7.66 (d, *J* = 7.4 Hz, 2H).

*Synthesis of **III-A***. *n*-BuLi (14.8 mL, 35.6 mmol) was added dropwise into a solution of **II-A** (3.03 g, 8.47 mmol) in anhydrous THF at −78°C under nitrogen atmosphere, and ethyl 2,2,2-trifluoroacetate (1.82 mL, 15.2 mmol)was added dropwise to the solution. Then, the resulting mixture was allowed to warm up to room temperature to react for 12 h. The reaction mixture was quenched by pouring into water and extracted with ethyl acetate. The combined organic layers were washed with water and dried over Na_2SO_4 and evaporated. The residual product was purified by flash column chromatography (silica gel, hexane/DCM = 3:1, v/v) to give **III-A** in a yield of 66% as a white powder. ^{1}H NMR (400 MHz, $CDCl_3$) δ (ppm): 0.92 (m, 3H), 0.96-1.18 (m, 2H), 1.29-1.37 (m, 4H), 1.44-1.59 (m, 3H), 1.88-2.01 (m, 4H), 2.72 (m, 1H), 7.37 (d, *J* = 8.0 Hz, 4H), 7.75 (d, *J* = 7.4 Hz, 2H), 7.99 (d, *J* = 7.4 Hz, 2H).

*Synthesis of **3HBBTfV***. t-BuOK (922 mg, 8.24 mmol) was added slowly to a solution of CH_3PPh_3Br (3.13 g, 8.97 mmol) in an ice bath of anhydrous THF (50 mL) under nitrogen atmosphere. After 2 h reaction, a solution of compound **III-A** (2.06 g, 5.49 mmol) in anhydrous THF (15 mL) was added dropwise to the previous reacted solution, and then the ice bath was removed. The solution was stirred to react for 4 h at room temperature. The reaction was terminated by concentrated HCl and extracted with ethyl ether. The combined organic layers were washed with water and dried over Na_2SO_4 and evaporated. The residual product was purified by recrystallization with hexane to give **3HBBTfV** in a yield of 70% as a white powder. ^{1}H NMR (400 MHz, $CDCl_3$) δ (ppm): 0.91 (m, 3H), 0.94-1.16 (m, 2H), 1.27-1.33 (m, 4H), 1.46-1.56 (m, 3H), 1.89-1.96 (m, 4H), 2.53 (tt, *J* = 12.0, 4.0 Hz, 1H), 5.84 (s, 1H), 5.98 (s, 1H), 7.31 (d, *J* = 8.0 Hz, 2H), 7.53-7.54 (m, 4H), 7.62 (d, *J* = 8.0 Hz, 2H). EI-MS (*m*/*z*) calcd for $C_{24}H_{27}F_3$ $[M]^+$, 372.2; found, 372.2. Anal. Calcd for $C_{24}H_{27}F_3$: C, 77.39; H, 7.31. Found: C, 77.51; H, 7.38. Tm = 151.8°C.

*2.3. Preparation of LC mixtures **A**, **B**, and **C***

LC mixture **A** was prepared from eight commercial molecular components, and their chemical structures and composition are shown in Table 1. LC mixture **A** was mixed with 10 wt% of **3HBEBTf** and **3HBBTfV** to obtain LC mixtures **B** and **C**, respectively.

#232681 - $15.00 USD Received 16 Jan 2015; revised 26 Feb 2015; accepted 1 Mar 2015; published 12 Mar 2015

3. Characterization and measurements

^{1}H NMR spectra were recorded on a Bruker DRX-400 (400 MHz) spectrometer using $CDCl_3$ as solvent. The EI-MS experiment was performed on a Bruker APEX II. All samples of homogeneous LC mixtures were filled into glass cells by capillarity. The LC cells were assembled in standard 90° twisted-nematic liquid crystal (TN-LC) configuration cells (crossed rubbing) and the thickness of liquid crystal layer was 4 μm. The UV aging experiments of LC materials were performed by means of an Atlas UV 2000 test machine (0.55 W/m^2, 365 nm) or a high power Rayonet UV reactor system (wavelength = 254 nm with an illumination energy > 50W/m^2). The UV exposure condition of TN-LC cells was followed by irradiating with UV light (0.55 W/m^2, 365 nm) at 50°C under 1 atm, in which the glass cells were cooled to room temperature and the VHR values of LCs were obtained. The values of VHR and response time along with voltage-transmission (*V-T*) characteristic curves of TN-LC cells were carried out by VHRM-105 and DMS-803 measurement systems (Autronic-Melchers GmbH). The clearing temperatures, melting points, and optical textures were studied using a polarizing optical microscope (POM, model: Olympus BX-51) equipped with a hot stage.

4. Results and discussion

The four-step synthetic route of UV-resistant dopant **3HBBTfV** is shown in Fig. 2. The chemical structure and purity of dopant **3HBBTfV** were confirmed by ^{1}H NMR and MS spectroscopies. Detailed synthetic procedures and characterization data are given in the experiment section. Both dopants **3HBEBTf** and **3HBBTfV** do not exhibit any mesophasic behavior and only show melting points at 98.0°C and 151.8°C, respectively. As demonstrated in Table 1, LC mixture **A** possessing the nematic phase at room temperature was selected as the LC host, which is composed of eight commercial molecular components. As given in Table 2, the clearing temperatures (T_cs) of LC mixture **A** (host), LC mixture **B** (**A**:**3HBEBTf** = 9:1 w/w), and LC mixture **C** (**A**:**3HBBTfV** = 9:1 w/w) are 75.0°C, 75.4°C and 80.8°C, respectively. The order of T_c values for all LC mixtures (i.e., LC Mixture **C** > **B** > **A**) are attributed to the contributions from their sequence of melting temperatures for dopants **3HBEBTf** and **3HBBTfV** in contrast to LC mixture **A** (host). Due to the highest rigidity of the direct coupling of three-ring structures in **3HBBTfV**, LC mixture **C** possesses the highest T_c value among all LC mixtures.

As demonstrated in Fig. 3, LC mixture **C** only displayed the nematic phase with the schlieren texture at room temperature in the POM study during cooling from the clearing temperature to room temperature. However, LC mixture **C** did not reveal any phase separation between dopant **3HBBTfV** and LC mixture **A** (host), which sufficiently indicated a good miscibility of the dopant material (**3HBBTfV**) in the host for LC mixture **C**. On the other hand, similar mesomorphic behavior was also observed in LC mixture **B**. The optical anisotropy Δn values of these LC mixtures are in the range of 0.1251–0.1275 (see Table 2).

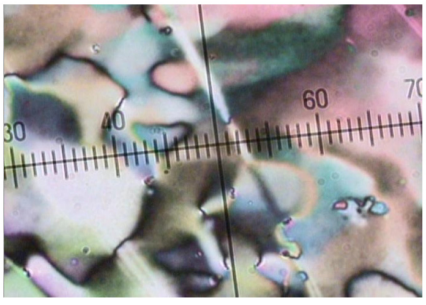

Fig. 3. Polarizing optical microphotograph of LC mixture C exhibited Schlieren texture in the nematic phase at room temperature between untreated glass plates.

#232681 - $15.00 USD Received 16 Jan 2015; revised 26 Feb 2015; accepted 1 Mar 2015; published 12 Mar 2015

Table 2. Thermal Properties and EO Characteristics[a] of LC Mixtures

Samples	T_c (°C)[d]	Δn	Δε	η (20°C, cps)
LC Mixture **A**	75.0	0.1275	4.974	14
LC Mixture **B**[b]	75.4	0.1271	5.103	15
LC Mixture **C**[c]	80.8	0.1251	5.167	13

[a] T_c = clear temperature (°C), Δn = birefringence, Δε = dielectric anisotropy, and η = viscosity, where the EO characteristics were measured at room temperature unless mentioned.
[b] LC Mixture **B** (**A**:**3HBEBTf** = 9:1 w/w), where **3HBEBTf** possesses Tm = 98.0°C.
[c] LC Mixture **B** (**A**:**3HBBTfV** = 9:1 w/w), where **3HBBTfV** possesses Tm = 151.8°C.
[d] Clearing temperatures were obtained by POM.

As shown in Fig. 4, the *V-T* cures of LC mixtures **A**, **B**, and **C** reveal gradual decreases in driving voltages sequentially in TN mode cells. The threshold-voltage (V_{th}) values of LC mixtures **A**, **B** and **C** are 1.25 V, 1.22 V, and 1.20 V, respectively, at 90% transmittance, as well as 2.25 V, 2.20 V, and 2.10V, respectively, at 10% transmittance. In comparison with the *V-T* curve of LC mixture **A**, both LC mixtures **B** and **C** have slightly reduced V_{th} values, which indicates that doping LC mixtures with **3HBEBTf** and **3HBBTfV**, respectively, are useful to improve the *V-T* curves with reduced V_{th} values. Moreover, due to the highest dielectric anisotropy of LC mixture **C** among all LC mixtures (Table 2), the lowest V_{th} value was induced by doping LC host with **3HBBTfV** (possessing a **TfV** moiety) in contrast to **3HBEBTf** (possessing a **BTf** moiety).

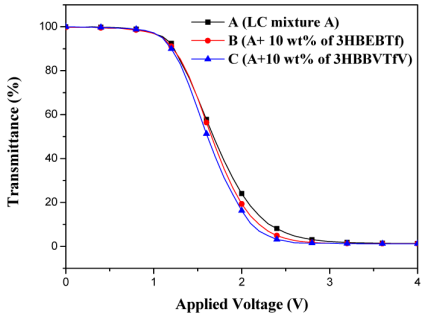

Fig. 4. *V-T* curves of LC mixtures A, B, and C in TN cells.

Since no obvious changes of *V-T* curves by UV irradiations at wavelength = 365 nm in all LC mixtures, the UV-resistant effects on *V-T* curves were accelerated under 2.5 h of UV exposure at wavelength = 254 nm with an illumination energy > 50W/m^2 to provide important implications regarding long-term UV stabilities of LC mixtures. The *V-T* curves of LC mixtures **A**, **B**, and **C** before and after UV exposure at wavelength = 254 nm (with a higher energy) are shown in Figs. 5(a), 5(b), and 5(c), respectively. As demonstrated in Fig. 5(b), a large discrepancy was observed in the *V-T* curves of LC mixture **B** before and after UV exposure. Comparably, after UV exposures Figs. 5(a) and 5(c) exhibited closer (almost overlapped) *V-T* curves of both LC mixtures **A** and **C**, which indicate more durable UV exposure properties were obtained while LC host **A** exited alone or mixed with UV-resistant **3HBBTfV**. According to the result of $V_{th} \fallingdotseq \pi(K_{11}/\varepsilon_0\Delta\varepsilon)^{1/2}$ [23], since the potential breakages of **3HBEBTf** and **3HBBTfV** under UV exposure are the ester linage of fluorobenzene (**BTf**) and the vinyl group of α-trifluomethyl vinylbenzene (**TfV**), respectively, the elastic constant reduction (K_{11}) in **3HBEBTf** is larger than **3HBBTfV** (but with little difference in both anisotropic dielectric constants Δε). As illustrated in Fig. 5(b), this result caused the largest reduction shift of V_{th} in LC mixture **B** containing **3HBEBTf** after UV exposure [34]. However, the breakage of the vinyl group in UV-resistant **3HBBTfV** maintained its elastic constant value (K_{11}) after UV exposure but reduced its anisotropic dielectric constant Δε. Thus, as displayed in Fig. 5(c) a small increasing shift of V_{th} in LC mixture **C** containing **3HBBTfV** was observed after UV exposure.

#232681 - $15.00 USD Received 16 Jan 2015; revised 26 Feb 2015; accepted 1 Mar 2015; published 12 Mar 2015

(a)

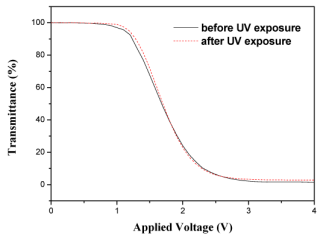

(b)

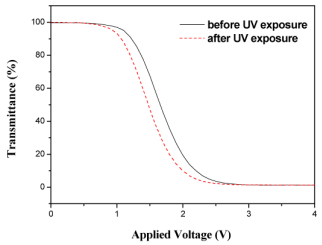

(c)

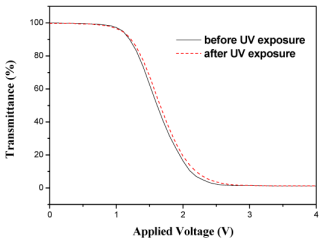

Fig. 5. *V-T* curves of (a) LC mixture A, (b) LC mixture B, and (c) LC mixture C in TN cells before and after UV exposure, where the UV exposure was proceeded at wavelength =254 nm with an illumination energy > 50W/m2 for 2.5 h.

Moreover, the response time (rise time τ_r, fall time τ_f, and total time τ_{total}) values of all LC mixtures were measured and compared. As illustrated in Table 3, the values of response time were increased from 6.9 to 7.2 ms to 7.1-7.6 ms, respectively, by UV exposure for all LC mixtures. However, the response time of LC mixture **C** had the smallest increment after UV exposure, which again suggested the contribution of the UV-resistant dopant **3HBBTfV** to LC mixture **C**.

Table 3. Response Time Values (τ_r, τ_f, and τ_{total}) of LC Mixtures[a]

	Before UV exposure			After UV exposure[b]		
Response time[c]	Host **A**	Mixture **B**	Mixture **C**	Host **A**	Mixture **B**	Mixture **C**
τ_r (ms)	1.6	1.8	1.7	1.9	1.9	1.6
τ_f (ms)	5.5	5.4	5.2	5.7	5.7	5.5
τ_{total} (ms)	7.1	7.2	6.9	7.6	7.6	7.1

[a] The response time experiments were measured at room temperature under the condition of a square-wave with a frequency of 120 Hz and Vrms = 6 volts.
[b] The UV exposure was proceeded at wavelength = 254 nm with an illumination energy > 50W/m^2 for 2.5 h.
[c] The response time values of rise time, fall time, and total time are τ_r, τ_f, and τ_{total}, respectively.

#232681 - $15.00 USD Received 16 Jan 2015; revised 26 Feb 2015; accepted 1 Mar 2015; published 12 Mar 2015

In addition, the voltage holding ratio (VHR) values of all three LC mixtures were evaluated after UV exposure, where the VHR value was defined as the ratio of the relaxed voltage in the non-selected period (V) to the initially selected voltage (V_o) at a specified frequency f (where V_o = 3.5 V and f = 60 Hz in this study), i.e., VHR = V/V_o [35]. As shown in Fig. 6(a), LC mixture **C** (mixed with **3HBBTfV**) showed a higher VHR value than LC mixtures **A** and **B** after UV exposure (365 nm, 0.55 W/m^2, 12 h). The VHR value of LC mixture **C** was barely decayed from > 99.5% to 98.9%, but it dropped to 68.7% for LC mixture **B** after 12 h of UV exposure. To accelerate this experiment, the UV exposure was proceeded again in a Rayonet UV reactor which provided 2.5 h of UV light (wavelength = 254 nm) with an illumination energy > 50W/m^2. As shown in Fig. 5(b), the result revealed that the VHR value of LC mixture **C** was hardly decayed from > 99.5% to 91.5% after 2.5 h of UV exposure, but it rapidly dropped to 11.5% for LC mixture **B** after 0.5 h of UV exposure. According to the previous report [36], the un-stabilities of the ester linkage and the fluorine substituents on the phenyl ring in the commercial component **3HBEBTf** containing a 3,4,5-trifluorobenzene (**BTf**) moiety can reduce their UV resistance [23]. Hence, the largest decays in VHR values of LC mixture **B** in Figs. 6(a) and 6(b) were due to the dissociation of LC mixtures **B** containing **3HBEBTf** after UV irradiations, which might generate new ionic species to reduce the relaxed voltages in the non-selected period (V) and thus to have smaller VHR values [37]. Therefore, LC mixture **C** (i.e., LC mixture **A** mixed with 10% wt. of **3HBBTfV**) was confirmed to possess the best UV light resistance among these LC mixtures.

(a)

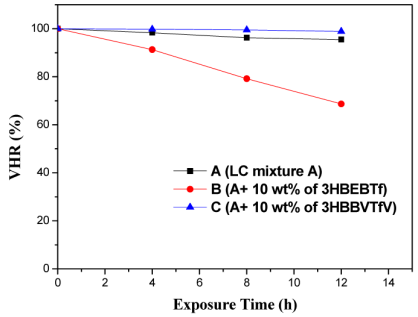

(b)

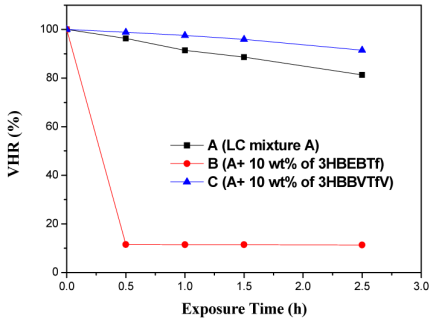

Fig. 6. VHR trends of LC mixtures A, B, and C in TN cells under exposures of (a) UV light (365 nm, 0.55 W/m2, 12 h) and (b) Rayonet UV reactor system (254 nm, > 50W/m2, 2.5 h), respectively.

4. Conclusion

In this study, a novel UV-resistant dopant **3HBBTfV** has been successfully designed and synthesized, which was well mixed with LC mixture **A** (as a host) to develop LC mixture **C**

#232681 - $15.00 USD Received 16 Jan 2015; revised 26 Feb 2015; accepted 1 Mar 2015; published 12 Mar 2015

and exhibited a high stability under UV exposure. By adding the UV-resistant dopant **3HBBTfV**, LC mixture **C** possessed the highest dielectric anisotropy $\Delta\varepsilon$ and the lowest viscosity η, and thus to reveal the best EO performance among all LC mixtures **A**, **B**, and **C**. Compared with analogous LC mixture **B** containing a commercial component **3HBEBTf**, this investigation showed that more stable VHR values of LC mixture **C** were still sustained after the UV irradiation. Therefore, dopant **3HBBTfV** (acting as an UV stabilizer) provides a reliable UV stability and better EO performance in contrast to the commercial component **3HBEBTf**. These EO performance results of LC mixture **C** containing the newly developed UV-resistant dopant **3HBBTfV** may have significant contributions to the LC researches and applications, especially for the LC mixtures required for the UV process (such as the photo-alignment under UV).

Acknowledgments

The financial supports provided by the Ministry of Science and Technology (MOST) of Taiwan (ROC) through MOST 103-2113-M-009-018-MY3 and MOST 103-2221-E-009-215-MY3 are acknowledged for this project. The electro-optical measurements were supplied by the Industrial Technology Research Institute (ITRI) in Hsinchu, Taiwan.

#232681 - $15.00 USD Received 16 Jan 2015; revised 26 Feb 2015; accepted 1 Mar 2015; published 12 Mar 2015